

# TIME-FREQUENCY LOCALIZED CDMA FOR DOWNLINK MULTI-CARRIER SYSTEMS

Anders Persson, Tony Ottosson, and Erik Ström

Department of Signals and Systems  
Chalmers University of Technology  
SE-412 96 Göteborg, Sweden

## ABSTRACT

An OFDM-CDMA system that utilizes the channel-correlation in both time and frequency to reduce multiple access interference is proposed. Orthogonal Walsh-Hadamard codes are used for spreading and in order for the codewords to stay orthogonal at the receiver, the channel response must be flat in both time and frequency. A frequency selective fading channel will, however, distort the codewords and thus introduce correlation. The proposed system, named Time-Frequency Localized CDMA (TFL-CDMA), places the codeword-chips in rectangular blocks on the time-frequency-grid in a such a way that the difference in scaling of the codeword chips is reduced. The proposed system is found to outperform competing schemes, such as Multi-Carrier (MC) and Multi-Carrier Direct-Sequence CDMA (MC-DS), in terms of bit error rate. The MC- and MC-DS-CDMA systems are special cases of the proposed scheme.

## 1. INTRODUCTION

In a traditional Direct-Sequence CDMA system signals are separated by user specific spreading codes, designed to have low correlation. The spreading is performed in the time domain, and the resulting signal is transmitted on a single carrier, see figure 1a. For downlink transmission, where signals can be transmitted synchronously, the orthogonal Walsh-Hadamard codes are often used. The orthogonality is however destroyed by a frequency selective channel. This effect, known as inter-path-interference, can severely degrade the performance. An OFDM system transmits with a lower rate on several parallel narrowband sub carriers so that each carrier is subject to approximately flat fading [1]. By using a cyclic prefix the sub carriers can be made orthogonal and the inter-symbol interference negligible. Placing the CDMA-chips on different carriers therefore ensures low inter-chip interference. Another advantage is that, as opposed to a single carrier DS-CDMA system, there is no need for a RAKE-receiver to resolve the time disperse channel. As a consequence there is also no need to find the exact positions of individual channel taps. Despite big implementation challenges, like designing linear amplifiers to cope with the large Peak-to-Average-Power ratio of an OFDM signal, multi carrier schemes are promising and has been subject to intensive research over the years, [2–4]. The earlier proposed Multi-Carrier CDMA (MC-CDMA) and Multi-Carrier Direct-Sequence CDMA (MC-DS-CDMA) systems spread the symbols either in the frequency or in the time direction [3]. These schemes are illustrated in figures 1c and d. A frequency selective fading channel will scale the chips differently and cause correlation between the codewords.

As will be seen in this paper, these schemes therefore easily become interference limited.

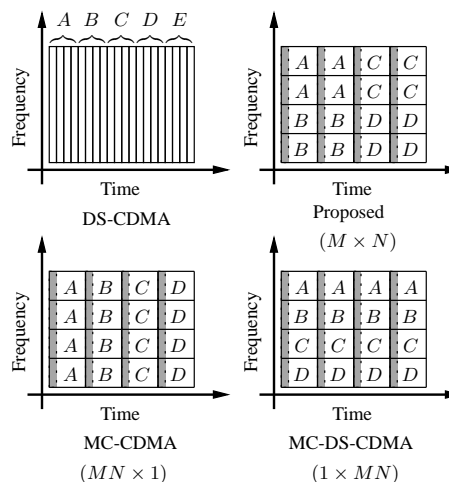


**Fig. 1.** Spreading in different CDMA systems. Figure a illustrates a wide-band single carrier system. The schemes in figure b, c and d are multi-carrier systems, where each column of the time-frequency grid corresponds to one OFDM-symbol. Each rectangle denotes one CDMA-chip and the letters  $A - E$  represent different codewords.  $M$  and  $N$  denotes the amount of spreading in the frequency and time direction respectively of the proposed system. Due to the cyclic prefix (gray regions) the multi-carrier schemes occupy more time-frequency resources compared to the DS-CDMA scheme.

## 2. THE PROPOSED SYSTEM

The proposed system utilizes the fact that the channel is correlated in both time and frequency, see figure 5. The codewords are localized to rectangular areas in order to reduce the difference in scaling among the chips. Let  $M$  and  $N$  denote the spreading in the frequency and time direction respectively of the proposed system. The MC- and MC-DS-CDMA systems can now be viewed as the  $(MN \times 1)$  and  $(1 \times MN)$  special cases of the proposed scheme. A block-scheme of the transmitter of the proposed system is shown in figure 2. The  $k$ th users information bits,  $b_k$ , are convolutionally encoded by the encoder labeled CC, interleaved by the pseudo-random-interleaver  $\Pi$  and thereafter QPSK-modulated. Thereafter traditional traditional direct-sequence spreading is applied, where

$c_k$  denotes the spreading code of user  $k$ . The different users' signals,  $s_k$ , are summed up prior to the block-shaping. The block-shaping operation places the codeword-chips in  $(M \times N)$  sized blocks on the time-frequency grid as illustrated in figure 1 b. The first  $M$  chips of the codeword are placed in the first column of the size  $(M \times N)$  matrix, the next  $M$  in the second column, and so on. The interleaver provides interleaving in both time and frequency, i.e., it makes the position of each  $(M \times N)$  block (encoded bit) on the grid pseudo-random. Several blocks per user are transmitted in parallel so that, as opposed to in a frequency hopped CDMA system, each user constantly occupies the entire bandwidth.

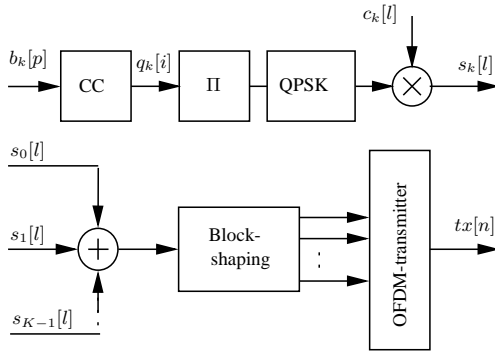


**Fig. 2.** Transmitter block-scheme of the proposed system.

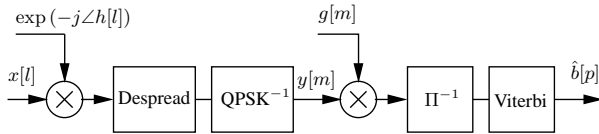


**Fig. 3.** Correlator, demodulator, deinterleaver and decoder.

The transmitter can be divided into a traditional DS-CDMA scheme with interleaving and channel coding, followed by the proposed block-shaping and a traditional OFDM transmitter. A rate  $-1/2$  convolutional code with a memory of 6 bits and generator polynomials  $\{133, 171\}$  given in octal format is used. Walsh-Hadamard codes of length  $MN = 64$  are used for the direct-sequence spreading. The total spreading of the DS-CDMA part of the scheme now becomes  $T_{b_k}/T_{s_k} = 2 \cdot \frac{1}{2} \cdot 64 = 64$ , where  $T_{b_k}$  and  $T_{s_k}$  denotes the bit and chip time respectively. The OFDM transmitter uses a 256-point IFFT, a main carrier frequency of 2 GHz and a sub carrier spacing of 15.625 kHz. A  $4 \mu\text{s}$  guard interval (cyclic prefix) is inserted. The resulting OFDM symbol time is  $68 \mu\text{s}$  and the system bandwidth approximately 4 MHz. The main carrier frequency and system bandwidth are thus similar to those of the UMTS system. One can argue that the cyclic prefix also contributes to the total spreading. Taking it into account yields a total spreading of  $T_{b_k}/T_{tx} = 2 \cdot \frac{1}{2} \cdot 64 \cdot \frac{68}{68-4} = 68$ , where  $T_{tx}$  is the sample output time (no oversampling is assumed).

### 3. CHANNEL MODEL

A frequency selective fading channel, modeled as a time varying FIR-filter [5, p. 797], is used in the performance evaluation of the proposed system, see figure 4. The channel taps are modeled as

independent complex Gaussian processes (Rayleigh fading), having the power spectra described in [6, p. 20]. The power-delay profile, shown in table 1, is chosen according to the standardized test channel *Vehicular Reference Environment A*, [7, p. 37].

delay [ns]	{0, 310, 710, 1090, 1730, 2510}
mean power [dB]	{0, -1, -9, -10, -15, -20}

**Table 1.** Power-delay profile for the Vehicular A channel. Delay and mean power relative the strongest tap.

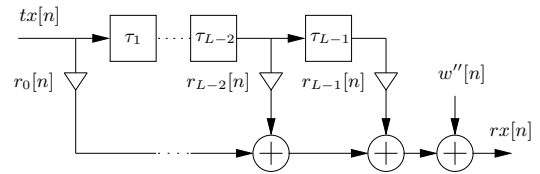


**Fig. 4.** Frequency selective channel.

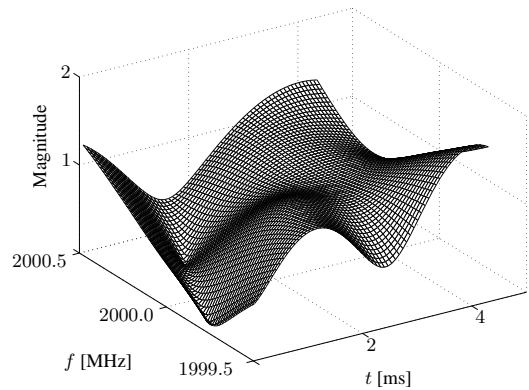


**Fig. 5.** Envelope of the complex valued time-frequency channel response  $H$ . A realization of the “Vehicular A” channel at a carrier frequency of 2 GHz and a mobile speed of 50 km/h.

### 4. PERFORMANCE EVALUATION

The performance is evaluated in a downlink scenario, where users are likely to request different transmitted powers in order to compensate for multiple access interference as well as their individual path losses. To illustrate the robustness of the proposed TFL-CDMA system to this so called near-far situation, the user that is decoded is given a received power that is either 5, 7.5 or 10 dB below each of the remaining active users within the cell. The average received  $E_b/N_0$  is, before the removal of the cyclic prefix, in all cases set to 8 dB. All figures show the performance at full system load, i.e.,  $K = 64$  active users. Except for in figure 9, the mobile speed is always set to 50 km/h. The optimal detector is the maximum likelihood sequence detector that jointly detects the different users signals. However, the complexity of this detector grows exponentially with the number of users and is, especially in the downlink, unrealistic with today's hardware. Therefore, sub optimal single user detectors are considered in this paper. A traditional OFDM-receiver followed by an operation that performs the

inverse to the earlier described block-shaping, yields the signal  $x$  that enters the block diagram of figure 3. Thereafter channel phase compensation, despreading and demodulation is performed. The output from the QPSK-demodulator for user 0 can be written

$$\begin{aligned}
y_0[m] &= \sqrt{\xi_0} q_0[m] \underbrace{\sum_{l=mS}^{(m+1)S-1} c_0^2[l] |h[l]|}_{\alpha[m]} + \\
&+ \underbrace{\sum_{k=1}^{K-1} \sqrt{\xi_k} q_k[m]}_{z[m]} \underbrace{\sum_{l=mS}^{(m+1)S-1} c_k[l] c_0[l] |h[l]|}_{z[m]} + \underbrace{\sum_{l=mS}^{(m+1)S-1} w'[l] c_0[l]}_{w[m]} \\
&= \sqrt{\xi_0} q_0[m] \alpha[m] + z[m] + w[m]. \quad (1)
\end{aligned}$$

Here  $\xi_k$ ,  $q_k$  and  $c_k$  denotes the chip energy, the encoded bits and the normalized spreading sequence of user  $k$  respectively.  $S = MN$  is the length of the direct-sequence spreading code. The two dimensional time-frequency channel response  $H$ , see figure 5, is after the inverse block shaping denoted  $h$ . Assume that the intra-cell-interference  $z$  as well as the additive receiver noise  $w$  in equation (1) is Gaussian and independent from coded bit to coded bit (perfect interleaving). The single user maximum likelihood sequence detector, given  $\{y_0\}$  in equation (1), chooses the sequence of coded bits  $\{\hat{q}_0\}$  with elements  $q_0[i] \in \{+1, -1\}$  as

$$\begin{aligned}
\{\hat{q}_0\} &= \arg \max_{\{q_0\}} \exp \left( -\frac{1}{2} \sum_i \frac{(y_0[i] - \sqrt{\xi_0} q_0[i] \alpha[i])^2}{\sigma_z^2[i] + \sigma_w^2} \right) \\
&= \arg \max_{\{q_0\}} \sum_i \underbrace{\frac{\alpha[i]}{\sigma_z^2[i] + \sigma_w^2}}_{g[i]} \cdot y_0[i] \cdot q_0[i] \quad (2)
\end{aligned}$$

The mapping between the information bits  $\{\hat{b}_0\}$  and the coded bits  $\{\hat{q}_0\}$  is determined by the convolutional code. The receiver is implemented by a standard Viterbi decoder that maximizes the correlation between the pre-weighted input  $\{g \cdot y_0\}$  and the hypothesis sequence  $\{q_0\}$ , see figure 3. The relation between the time indexes  $m$  and  $i$  is determined by the interleaver  $\Pi$ . From equation (2) it is seen that the sequence of weights,  $\{g\}$ , should be chosen as

$$g[i] = \frac{\alpha[i]}{\sigma_z^2[i] + \sigma_w^2}. \quad (3)$$

Choosing  $\{g\}$  as in equation (3) requires knowledge of the channel envelope, the power of each interfering user and the variance of the receiver noise. A more practical approach is to disregard the interference part  $\sigma_z^2$  and to choose  $\{g\}$  as

$$g[i] = \alpha[i] \quad (4)$$

were the thermal noise now also can be disregarded since  $\sigma_w^2$  can be considered constant in time.

#### 4.1. Semi-analytical BER evaluation

The BER performance of a convolutional code can be upper bounded by a union bound [5, p. 488]

$$P_b \leq \sum_{d=d_f}^{\infty} c_d P_2(d) \quad (5)$$

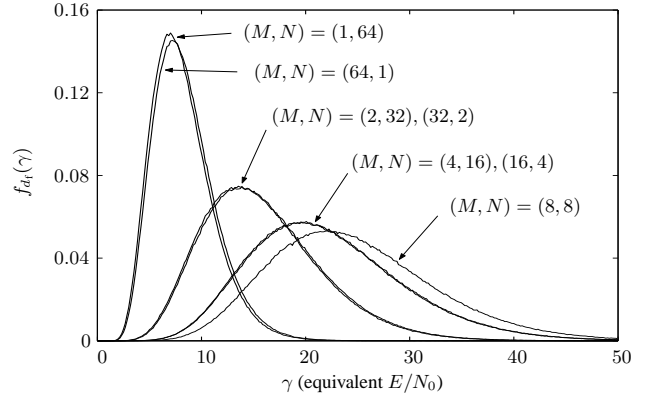


**Fig. 6.** Histogram based estimate of the pdf of the signal to interference plus noise ratio of 10 combined coded bits, (the free distance of the code is 10). The horizontal axis shows the equivalent  $E/N_0$  in linear scale. The soft metric weights are chosen as in equation (3), i.e. maximum ratio combining. The near-far ratio is 10 dB and the average received  $Eb/N_0$  is 8 dB.

where  $d_f$  is the free distance of the code,  $P_2(d)$  is the pair-wise error probability of two sequences separated by a Hamming distance  $d$ , and  $c_d$  is the information error weights of the code. An approximate value of the BER may be obtained by truncating the sum in equation (5) at some suitable  $d$ . To find an expression for  $P_2(d)$  in a fading scenario the error probability given the instantaneous signal to interference plus noise ratio,  $\gamma$ , should be averaged over the probability density function  $f_d(\gamma)$ . Assuming Gaussian interference and noise, yields the pair-wise error probability

$$P_2(d) = \int_0^{\infty} f_d(\gamma) Q(\sqrt{2\gamma}) d\gamma. \quad (6)$$

Using the soft metric weights in equation (3) results in maximum ratio combining. A closed form expression for  $f_d(\gamma)$  has not been found in this case. Histogram estimates of the pdf can however be used, see figure 6. These are obtained from computer realizations of the sum of  $d$  independent variables  $\gamma_c$  generated according to equation (7).

$$\gamma_c = \frac{\alpha^2[i]}{\sigma_z^2[i] + \sigma_w^2} \quad (7)$$

Although the analysis now becomes partly based on computer simulations, it serves as a method of validating the full Monte-Carlo simulation.

#### 4.2. Computer simulations

Monte-Carlo simulations of the proposed system using different spreading block shapes  $(M, N)$  were performed. The main goal of this performance evaluation is to illustrate the potential gains that result from reduction of MAI, due to the block shaping operation. In order to isolate this phenomena as much as possible imperfections, such as diversity limitations due to insufficient interleaving, has to be avoided. For this reason, the simulations are performed with an interleaver size of approximately 20000 coded bits ( $\approx 0.15$ s). A system with real time demands would have to use a significantly smaller interleaver. Perfect synchronization and perfect channel estimates were also used.

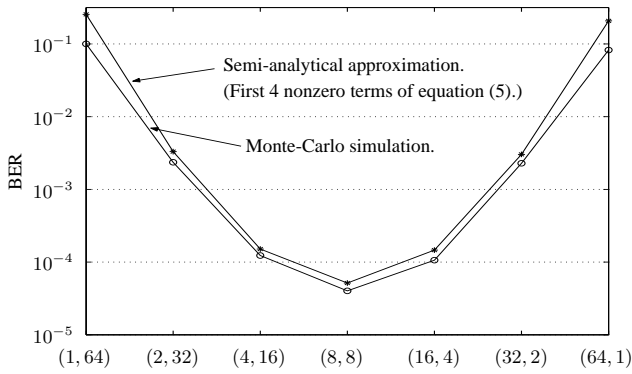


**Fig. 7.** Bit error rate at a near-far ratio of 10 dB for different block shapes  $(M, N)$  when using the soft metric weights in equation (3). The average received  $E_b/N_0$  equals 8 dB. The earlier proposed MC- and MC-DS-CDMA systems correspond to the  $(64, 1)$  and  $(1, 64)$  shapes respectively.

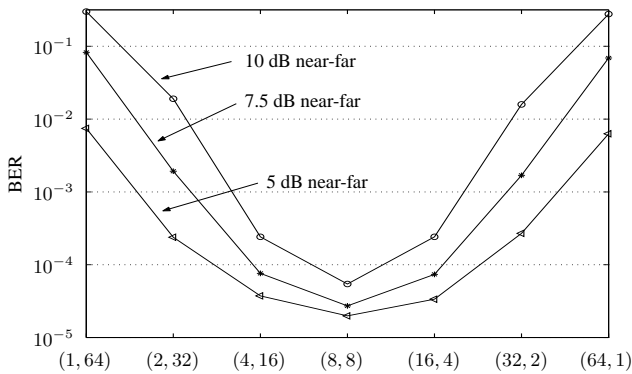


**Fig. 8.** Computer simulation of the bit error rate for different block shapes,  $(M, N)$ , at different near-far ratios and an  $E_b/N_0$  of 8 dB. Soft metric weighting according to equation (4).

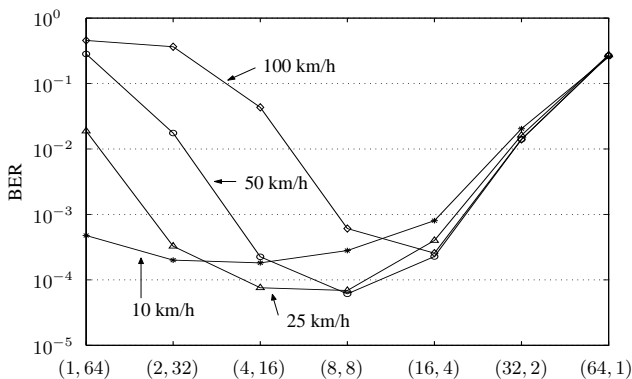


**Fig. 9.** Computer simulations of the bit error rate at a near far ratio of 10 dB for different block shapes,  $(M, N)$ , and different mobile velocities. Soft metric weighting according to equation (4) and an  $E_b/N_0$  of 8 dB.

## 5. DISCUSSION AND CONCLUSIONS

The earlier proposed MC- and MC-DS-CDMA systems correspond to the  $(MN, 1)$  and  $(1, MN)$  special cases of the proposed TFL-CDMA scheme. Localizing the codewords on the time-frequency grid suppresses the intra-cell-interference that results from codeword distortion. Placing the codewords non-localized, like in the MC- and MC-DS-CDMA systems, yields severe interference problems, but on the other hand ensures lower probability of placing the entire codeword in a deep fade. The choice of block shape is thus a trade-off between either obtaining interference suppression or diversity gains. However, in a downlink CDMA scenario, the overall system performance (number of simultaneously supported users at a certain bit rate) is in most situations limited by intra- and inter-cell-interference. Increased near-far robustness (lower correlation between codewords) reduces the amount of power necessary to maintain a certain bit error rate. As a consequence, also the amount of interference power experienced by other users in the system is reduced, and a significant increase in overall system performance can be expected. From figure 7-9 it is concluded that both the MC- and MC-DS systems are outperformed by the proposed scheme in a near-far scenario. From a comparison of figure 7 and 8 it is concluded that the loss in BER performance when using the soft metric weights in equation (4) rather than the maximum ratio weights in equation (3) is small. The preferred shape of the spreading block varies with the statistical properties of the channel. The proposed solution is however found to be robust to different Doppler frequencies (mobile speeds), see figure 9. The increase in bit error rate in the 10 km/h case is likely caused by the diversity loss due to the slowly time varying channel (insufficient interleaving). No power control scheme, that partly can compensate for slowly time varying channels, is used in the simulations. A thorough study involving different power-delay profiles and mobile velocities is needed, as well as a fully analytical performance evaluation. Also, the use of the proposed scheme in a quasi-synchronous uplink, where comparable performance gains can be expected, is a topic for future research [4].

## 6. REFERENCES

- [1] R. Van Nee and R. Prasad, *OFDM For Wireless Multimedia Communications*, Artech House, 2000.
- [2] D. Lee and L. B. Milstein, "Comparison of Multicarrier DS-SS-CDMA Broadcast Systems in a Multipath Fading Channel," *IEEE Transactions on Communications*, vol. 47, no. 12, pp. 1897–1904, Dec. 1999.
- [3] S. Hara and R. Prasad, "Design and Performance of Multicarrier CDMA Systems in Frequency-Selective Rayleigh Fading Channels," *IEEE Transactions on Vehicular Technology*, vol. 48, no. 5, pp. 1584–1595, 1999.
- [4] Georgios B Giannakis, "AMOUR-Generalized Multicarrier Transceivers for Blind CDMA Regardless of Multipath," *IEEE Transactions on Communications*, vol. 48, no. 12, pp. 2064–2076, Dec. 2000.
- [5] J.G. Proakis, *Digital Communications, 3rd edition*, McGraw-Hill, 1995.
- [6] W. C. Jakes, Ed., *Microwave Mobile Communications*, IEEE Press, 1993, reissue.
- [7] J. P. Castro, *The UMTS Network and Radio Access Technology*, John Wiley & Sons, 2001.